

## An exchange flow between the Okhotsk Sea and the North Pacific driven by the East Kamchatka Current

Shinichiro Kida<sup>1</sup> and Bo Qiu<sup>2</sup>

Received 24 September 2013; revised 5 November 2013; accepted 20 November 2013.

[1] A new mechanism for driving the water mass exchange between the Okhotsk Sea and the North Pacific is presented. This exchange flow originates from the East Kamchatka Current (EKC), a western boundary current of the subpolar gyre, and occurs through the two deepest straits of the Kuril island chain, the Kruzenshtern and Bussol straits. An inflow toward the Okhotsk Sea occurs at the northern Kruzenshtern strait and an outflow toward the North Pacific occurs at the southern Bussol strait. By using the Kelvin's Circulation theorem around the island between the two straits, we show that the transport of the exchange flow entering the Okhotsk Sea is determined such that the frictional stresses around the island exerted by the bifurcated EKC integrate to zero. This forcing mechanism is different from the dynamical framework of the widely used "Island rule." Both an analytical analysis and 1.5-layer model experiments demonstrate that the strait width, lateral viscosity, and island geometry are controlling parameters for the exchange flow transport because they affect the magnitude and length scales of the frictional stresses. Inertia of the EKC decreases the exchange flow by enhancing the frictional stress along the northern coast of the Kuril island. Model experiments with realistic topography further reveal that while the steep continental slopes have minor impact on the exchange flow transport, the subsurface peninsula located east of the Kuril island works to decrease the exchange flow by altering the length scale of the frictional stresses and enabling the EKC to flow past the island.

**Citation:** Kida, S., and B. Qiu (2013), An exchange flow between the Okhotsk Sea and the North Pacific driven by the East Kamchatka Current, *J. Geophys. Res. Oceans*, 118, doi:10.1002/2013JC009464.

### 1. The Water Mass Exchange Between the Okhotsk Sea and the North Pacific

[2] The Okhotsk Sea is a marginal sea located at the north-west corner of the North Pacific. While this sea covers an area of more than  $4 \times 10^5$  km<sup>2</sup>, it is topographically separated from the North Pacific by the Kuril island chain. There are only two major gaps, the Kruzenshtern and Bussol straits, where the island chain permits an exchange flow (Figure 1). The Kuril island chain is therefore analogous to a thin wall that is only about 30 km wide zonally but a thousand kilometer long meridionally. While the magnitude of the exchange flow is limited, this flow plays an important role in the North Pacific from the regional to basin scale

circulations. The Okhotsk Sea water is considered one of the major sources of the North Pacific intermediate water [Talley, 1993; Yasuda, 1997] and iron that enables the high productivity in the region [Nishioka et al., 2007].

[3] The exchange flow between the Okhotsk Sea and the North Pacific originates from the East Kamchatka Current (EKC) [Yasuda et al., 2002]. The EKC is a western boundary current of the North Pacific subpolar gyre with a transport of about 10–11 Sv [Verkhunov and Tkachenko, 1992]. While part of the EKC enters the Okhotsk Sea, the majority of this flow continues along the eastern side of the island chain from the Kamchatka Peninsula to the Island of Hokkaido as a western boundary current of the North Pacific and becomes the Oyashio [Yasuda et al., 2002]. The exchange flow between the Okhotsk Sea and the North Pacific is observed to occur mainly across two major gaps where the island chain cracks more than 1000 m deep and 40 km wide. An inflow toward the Okhotsk Sea occurs at the Kruzenshtern Strait and an outflow toward the North Pacific occurs at the Bussol strait [Katsumata et al., 2001, 2004]. While variability of this exchange flow on the seasonal and tidal time scales has been observed, past studies suggest its annual averaged transport to be around 3–5 Sv [Yasuda et al., 2002; Nakamura and Awaji, 2004; Katsumata and Yasuda, 2010; Ohshima et al., 2010].

<sup>1</sup>Earth Simulator Center, Japan Agency for Marine-Earth Science and Technology, Yokohama, Japan.

<sup>2</sup>Department of Oceanography, University of Hawaii at Manoa, Honolulu, Hawaii

Corresponding author: S. Kida, Earth Simulator Center, Japan Agency for Marine-Earth Science and Technology, 3173-25 Showa-machi, Kanazawa-ku Yokohama, Kanagawa 236-0001, Japan. (kidas@jamstec.go.jp)

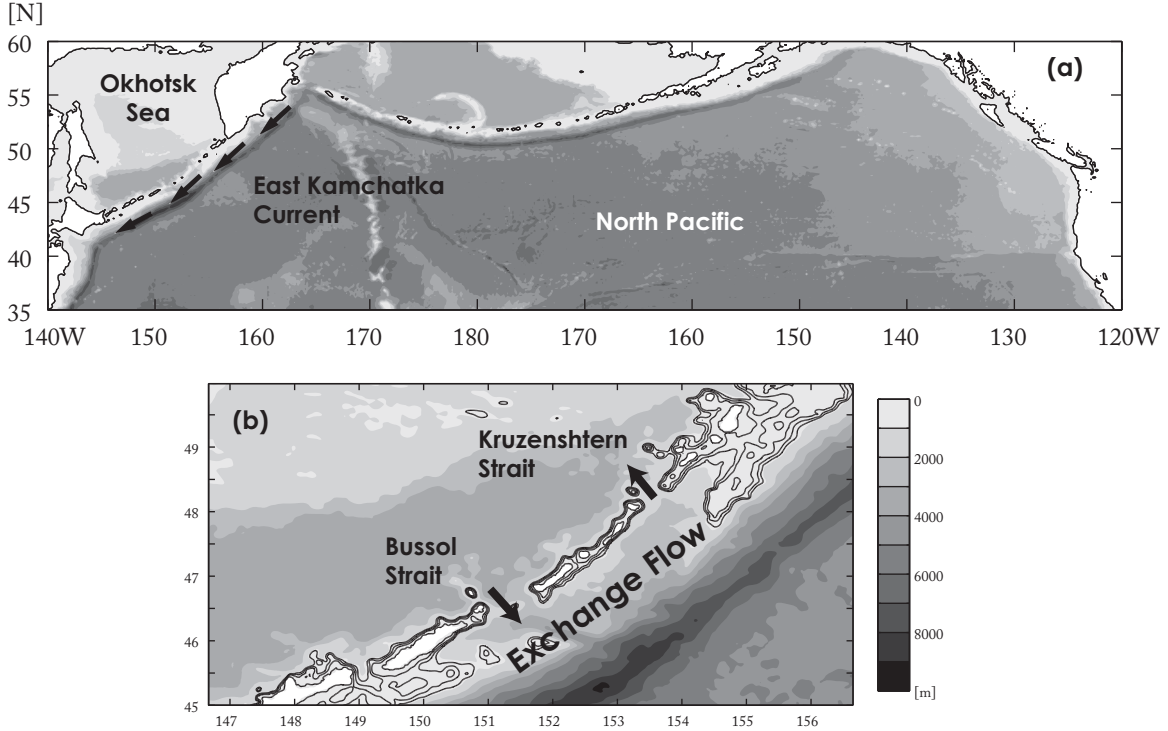


**Figure 1.** (a) The bathymetry and coastlines of the Okhotsk Sea and the North Pacific. The East Kamchatka Current flows along the Kuril island chain. (b) A closer look of the Kuril island chain. The exchange flow occurs through the Kruzenshtern strait and Bussol strait. Bathymetric contours shallower than 1000 m are drawn in black solid lines every 250 m.

### 1.1. The Mechanism of the Water Mass Exchange

[4] What are the main processes that drive the exchange flow between the Okhotsk Sea and the North Pacific?

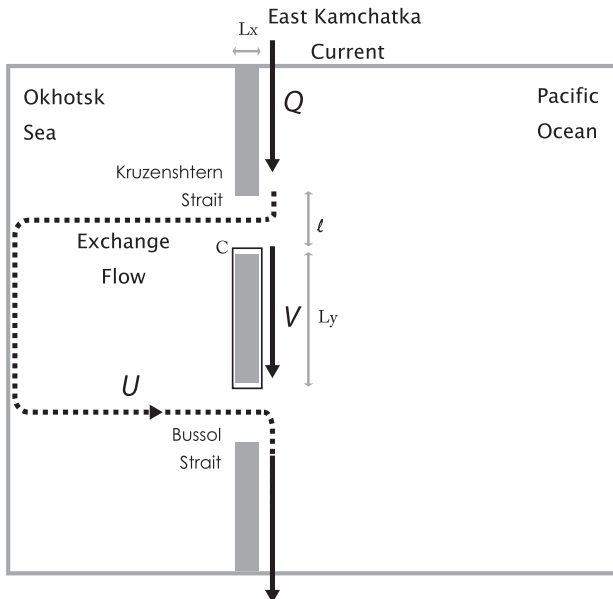


**Figure 2.** A schematic showing an exchange flow, the EKC, the Okhotsk Sea, and the North Pacific. Model parameters and the line integral  $C$  used in equation (1) are also shown.

Understanding its mechanism is important not only for understanding the oceanic environment of the Okhotsk Sea and its impact on the North Pacific but also for properly simulating this exchange flow in general ocean circulation numerical models. Latest high-resolution general circulation models (GCM) are only just beginning to resolve the width of the straits and permit an exchange flow.

[5] *Katsumata and Yasuda [2010]* and *Ohshima et al. [2010]* recently found that the transport of the exchange flow is likely correlated with that estimated from the Island rule [*Godfrey, 1989*] on the seasonal cycle. These studies imply that the open ocean winds are remotely driving the exchange flow. However, their studies also find the Island rule overestimating the transport by 1 order of magnitude. Since the original Island rule aims to estimate the magnitude of an exchange flow around an isolated island that is of planetary scale, direct application of such theory to the Kuril island chain may have been inappropriate. Moreover, the Island rule is based on a steady state assumption and is not applicable for the seasonal time scale. While the connection between the open ocean winds and the exchange flow may be qualitatively plausible, the actual mechanism that drives the exchange flow is still an open question.

### 1.2. The Goal of This Paper

[6] In this paper, we propose that the primary forcing agent of the exchange flow is the EKC. Since the EKC is a western boundary current of the subpolar gyre of the North Pacific, this EKC-driven mechanism is in line with the idea that the exchange flow is remotely driven by the open ocean winds. By using the Kelvin's Circulation Theorem, we show that the

presence of narrow straits plays an important role in determining how much of the EKC becomes the exchange flow.

[7] Detailed mechanism of the EKC-driven exchange flow, including how this mechanism is connected to the Island rule, will be explained first in section 2. Two sets of numerical models are then used to test our hypothesis: a 1.5-layer reduced gravity model and a two-layer isopycnal model. Detailed setup of these models is described in section 3. The basic dynamics of the EKC-driven exchange flow are examined using the 1.5-layer model and the simulation results, including various sensitivity experiments, are presented in section 4. The impact of bottom bathymetry is discussed in section 5 using the two-layer model. Summary and closing remarks are presented in section 6.

## 2. The Mechanism of an EKC-Driven Exchange Flow

### 2.1. An Exchange Flow Driven by a Western Boundary Current

[8] Let us consider an idealized case, where the North Pacific and the Okhotsk Sea are separated by two peninsulas and an island in between that mimics the Kuril island chain (Figure 2). The EKC is flowing southward along this island chain and the flow field is assumed to be in a steady state. As the EKC flows southward along the northern peninsula, it encounters the Kruzenshtern strait and bifurcates into a component that enters the Okhotsk Sea and the other that continues southward along the island. The flow that enters the Okhotsk Sea will circulate and rejoin the EKC at the Bussol strait. The rejoined EKC will then flow southward along the southern peninsula. If there were no island, there would be only one strait and the EKC that enters the Okhotsk Sea will come back out at the same strait. Such scenario is discussed in *Sheremet* [2001], where the dynamics of a western boundary current leaping across a strait is examined. If the Okhotsk Sea is infinitely long in the zonal direction, then the flow that enters this sea will continue westward and never return. Such scenario is discussed in *Nof* [1995], where an adjustment of a flow through a broad gap is examined with a focus on the Indonesian Throughflow. These two scenarios are, however, not directly applicable here because there are two straits and the flow that enters the Okhotsk Sea circulates and comes back out.

[9] Can we determine how much of the EKC enters the Okhotsk Sea when there are two straits with an island in between? In order to answer this question, we need to understand what causes the EKC to bifurcate. If the dynamics were inviscid [*Durland and Qiu*, 2003] or if the width of the two straits were wide such that the EKC does not touch the island as it turns westward (southward) at the northern (southern) strait, all of the EKC will enter and exit the Okhotsk Sea. No bifurcation occurs and the presence of an island plays no role on the flow field. However, if the straits are narrow and friction is nonnegligible, then the EKC will touch the island and exert a frictional stress on the northern and southern coasts of the island as it squeezes through the straits. This frictional stress will make the EKC bifurcate and establish an exchange flow along the straits and a boundary current along the eastern coast of the island.

[10] The reason why the EKC bifurcates when it exerts a frictional stress on the island can be shown from the

Kelvin's Circulation Theorem (Circulation theorem, hereafter). Based on the momentum equation integrated along an island:

$$\frac{\partial}{\partial t} \left( \oint_C \mathbf{u} \cdot d\mathbf{l} \right) = \oint_C [A_H \nabla \cdot \nabla \mathbf{u}] \cdot d\mathbf{l} + \oint_C \frac{\tau}{\rho} \cdot d\mathbf{l}, \quad (1)$$

where  $C$  is the line integral around an island (Figure 2), the Circulation theorem suggests that the sum of the frictional and wind stresses along an island (the two terms on the RHS) must balance the tendency of the flow along an island (the term on the LHS). The notations used in equation (1) are conventional.  $d\mathbf{l}$  is the unit vector tangent to the island.  $A_H$  is the lateral viscosity coefficient.  $\tau$  is the wind stress. For a steady state with no wind stress, the tendency and wind stress terms in equation (1) are zero. With the sole frictional stress term remaining, equation (1) indicates that the frictional stress along an island must integrate to zero:

$$0 = \oint_C [A_H \nabla \cdot \nabla \mathbf{u}] \cdot d\mathbf{l}. \quad (1')$$

Equation (1') implies that when the EKC enters/exits the straits and exerts frictional stresses along the northern and southern coasts of an island in a cyclonic sense, there must also establish a flow flowing along the western and eastern coasts in an anticyclonic sense so that the sum of the frictional stresses goes to zero. Since an eastern boundary current is unlikely to establish on a  $\beta$ -plane, a southward western boundary current is the one that will establish (Figure 2).

[11] Using equation (1'), we can further estimate the ratio of a steady EKC bifurcating into an exchange flow and a western boundary current along the eastern coast of the island. We will assume that the meridional length scale of the exchange flow along the northern and southern boundaries of the island to be  $l/2$ , where  $l$  is the width of the strait. The zonal length scale of the western boundary current is taken to be the Munk boundary layer width,  $\delta_M = (A_H/\beta)^{1/3}$  [e.g., *Pedlosky*, 1996]. Using the exchange transport  $U$ , the transport of the western boundary current along the eastern coast of the island  $V$ , the layer depth  $H_0$ , and  $L_x$  and  $L_y$ , the width and length of the island, respectively, the integral of the frictional stresses around the island in equation (1') can be scaled and expressed by:

$$\begin{aligned} 0 &= \oint_C [A_H \nabla \cdot \nabla \mathbf{u}] \cdot d\mathbf{l} \\ &= A_H \left( \frac{U/(H_0 \cdot l/2)}{(l/2)^2} L_x + \frac{(-V)/(H_0 \cdot \delta_M)}{\delta_M^2} L_y \right. \\ &\quad \left. - \frac{(-U)/(H_0 \cdot l/2)}{(l/2)^2} L_x \right). \end{aligned} \quad (2)$$

The first, second, and third terms in equation (2) are the frictional stresses exerted along the northern, eastern, and southern coasts of the island, respectively. We have

assumed that the flow along the western coast of the island is negligible. Equation (2) can then be expressed as:

$$0 = 16 \cdot \frac{U}{\beta} Lx - \frac{V}{\delta_M^3} Ly, \quad (3)$$

where equation (3) clearly shows that the Circulation theorem requires the magnitude of the exchange flow and island's western boundary current to depend on each other. By further using mass conservation ( $U+V=Q$ ), an estimate for  $U$  is derived:

$$U = \frac{Q}{1+16\alpha\gamma^{-3}}, \quad (4)$$

where  $\alpha$  is the aspect ratio of the island,  $L_x/L_y$ , and  $\gamma$  is the nondimensional width of the strait,  $l/\delta_M$ .

[12] Equation (4) shows that the exchange flow  $U$  is sensitive to two parameters,  $\alpha$  and  $\gamma$ , and that  $U$  decreases when  $\alpha$  increases or when  $\gamma$  decreases. This sensitivity of  $U$  on  $\gamma$  is similar to the sensitivity of a western boundary current leaping across a gap [Sheremet, 2001]. The sensitivity of  $U$  on  $\alpha\gamma^{-3}$  is similar to that of the Island rule when an

island is located close to a wall so that friction enhances along the northern or southern coasts of an island [Pedlosky et al., 1997]. Pratt and Pedlosky [1998] also discuss the role of friction based on the Island rule but in the absence of a western boundary current from the upstream. As will be further clarified in the next subsection, it is the presence of the western boundary current from the upstream in our case that drives the exchange flow in equation (4). For the exchange flow across the Kuril island chain, the EKC and two narrow straits enables us to derive equation (4) and evaluate the sensitivity of  $U$  more quantitatively. We will discuss how this EKC-driven mechanism and the Island rule are connected next.

## 2.2. The EKC-Driven Mechanism and the Island Rule

[13] Theoretical studies on flows around an island progressed much on what is known as the Island rule [Godfrey, 1989]. In this subsection, we will clarify how the mechanism of an EKC-driven exchange flow put forth in section 2.1, differ from, and connect to, this theory.

[14] One simple difference is in the forcing agent. The exchange flow in the EKC-driven mechanism requires a boundary current flowing from the upstream. It does not depend on whether a wind stress in the open ocean is present or not. On the other hand, the exchange flow in the Island rule is

$$U_{IR} = \frac{1}{\rho\beta(y_N - y_S)} \int_{y_S}^{y_N} \int_{x_E}^{x_W} \nabla \times \tau dx dy, \quad (5)$$

and requires a wind stress to be present east of an island (gray area in Figure 3a), [Pedlosky, 1996]. It does not depend, however, on the wind stress or flow field outside of this region.

[15] The second difference is that the EKC-driven mechanism assumes a different way of balancing the frictional stresses that are exerted around the island. For the EKC-driven mechanism, the frictional stress along the northern and southern coasts of the island balances that along the eastern coast. For the Island rule, the frictional stress balances within the eastern coast of the island. In other words, the frictional stresses along the northern, southern, and western coasts of the island are assumed zero while the total frictional stress around the whole island is also zero. The assumption that frictional stress balances within the eastern coast of an island is likely to be valid when the meridional length scale of the island is planetary and much larger than the zonal length scale of the island.

[16] The third, and most important, difference is that the EKC-driven mechanism considers the wind-driven Sverdrup flow congregating at the northern tip of the island as an incoming western boundary current (Figure 3b). No such congregation is considered in the Island rule. To clarify the relevance of this difference, we begin by discussing the Island rule in a rectangular basin with a cyclonic wind-driven gyre and an isolated island in the interior (Figure 3a).

[17] As equation (5) shows, the Island rule estimates the flow around an island based on the spatial average of the Sverdrup flow east of the island. However, it is also important to note that equation (5) contains a component of the

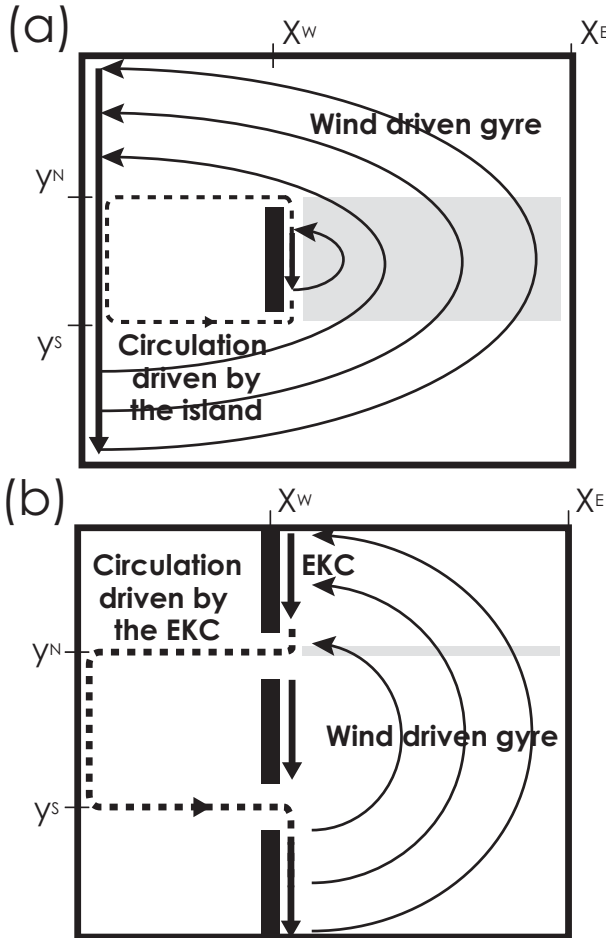


**Figure 3.** Two ways the open ocean wind drives an exchange flow: (a) the Island rule. The circulation driven around the island is determined by the Sverdrup balance within the gray area. (b) EKC-driven mechanism. The EKC is driven by the integral of the Sverdrup balance along the gray line.

wind-driven gyre that the presence of an island has no influence on. As mentioned by *Pedlosky et al.* [1997], the validity of equation (5) can be artificially improved by simply increasing the eastern domain size and increasing the component of the Sverdrup flow. What the Island rule illuminates is how an island perturbs the interior flow field from that driven in absence of the island. Such island-driven flow is shown as a dotted line in Figure 3a and its magnitude at  $y = y_N$  can be estimated by  $U_{IR} - Q$ , where

$$Q = \frac{1}{\rho\beta} \int_{x_w}^{x_e} \nabla \times \tau(y=y_N) dx \quad (6)$$

is the zonally integrated Sverdrup flow along the northern boundary of the island. If the northern boundary of the island is located where  $Q$  is close to zero [e.g., *Pedlosky*, 1994, Figure 3], then the flow around an island is driven solely due to the Island rule. However, if the meridional length scale of an island is small,  $U_{IR} - Q$  is likely small because the difference between the spatial average of the wind stress curl (equation (5)) and that along the northern latitude of the island (equation (6)) is likely small. The island-driven flow would be weak and what equation (5) expresses is simply the zonal transport of a Sverdrup balanced wind-driven gyre (the solid lines in Figure 3a). In this case of small  $U_{IR} - Q$ , it is probably best to regard the flow around the island,  $U_{IR}$ , as part of the wind-driven gyre and *not* as a flow driven by the presence of an island and dictated by the Island rule.

[18] The EKC-driven mechanism considers the case when an island is not an isolated island, but is bounded by two peninsulas (Figure 3b). In such situation, the Sverdrup wind-driven gyre circulation can no longer simply go around the island. A western boundary current will establish along the peninsula instead with a transport of  $Q$  at  $y = y_N$ . When the straits are narrow, this boundary current will touch the island and drive an EKC-driven exchange flow. Notice that  $Q$  would be dynamically irrelevant in the case of Figure 3a, but in the presence of a peninsula, it will interact directly with the island and affect the magnitude of the exchange flow. Such role of narrow straits is different from that discussed by *Pedlosky* [1994], *Pratt and Pedlosky* [1998], and *Pratt and Spall* [2003] in which the impact of narrow straits on the Island rule is examined. A western boundary current from upstream ( $Q$ ) is absent in these studies. What the EKC-driven mechanism highlights is a scenario when the Sverdrup component of the wind-driven gyre interacts directly with the island and plays a central role in determining the magnitude of the flow around an island.

[19] The EKC-driven mechanism and the Island rule complement each other for explaining the dynamics of a flow around an island. Their roles can be conceptually summarized by the following equation:

$$U_{Exchange} \approx (U_{IR} - Q) + \frac{Q}{1 + 16\alpha\gamma^{-3}}, \quad (7)$$

where  $U_{Exchange}$  is the total exchange transport around an island. The first term on the right denotes the island-driven

**Table 1.** The Basic Settings Used in the Numerical Experiments

Experiment	CTRL	NCTRL	SLOPE	RTOPO
Model	1.5 layer	1.5 layer	HIM	HIM
Topography			Constant slope	ETOPO2

flow, estimable from equations (5) and (6) and corresponds to the dotted line in Figure 3a. It assumes that the island is isolated. The second term is the exchange flow determined from the EKC-driven mechanism. It corresponds to the dotted line in Figure 3b and assumes that the island is bounded by two straits. If the straits are wide, all of the western boundary current from the upstream will flow through the straits so this second term becomes  $Q$  and cancels out with  $-Q$  in the first term. The original form of the Island rule (equation (5)) is then recovered:  $U_{Exchange} \sim U_{IR}$ . If the meridional length scale of an island is small and the straits are narrow (i.e., both  $l$  and  $U_{IR} - Q$  are small), the equation for the EKC-driven mechanism (equation (4)) is recovered:  $U_{Exchange} \sim Q/(1 + 16\alpha\gamma^{-3})$ . We expect that this latter scenario more appropriate for the exchange flow driven across the Kuril island chain. When  $U_{IR}$  and  $Q$  are estimated using the climatological annual mean QuikSCAT wind stress data [*Risien and Chelton*, 2008],  $U_{IR}$  is about 16 Sv and  $Q$  is about 21 Sv. While a positive  $U_{IR}$  value suggests a cyclonic circulation, its magnitude is much larger than that observed for the exchange flow [*Katsumata and Yasuda*, 2010; *Ohshima et al.*, 2010]. Moreover, the island-driven flow at the latitude of the Kruzenshtern trait,  $U_{IR} - Q$ , is in this case negative (cf. Figure 3a). These observational results support the notion that the exchange flow around the Kuril island chain is better understood as being EKC-driven, rather than determined by the classical Island rule.

### 3. Model Setup

[20] The details of the numerical model experiments are described in this section (Table 1). A 1.5-layer reduced gravity model is used for examining the basic mechanism of the EKC-driven exchange flow. A two-layer model is used for examining the impact of realistic bottom topography, which cannot be examined with a 1.5-layer model.

#### 3.1. 1.5-Layer Reduced Gravity Model

[21] The 1.5-layer reduced gravity model solves the following governing equations:

$$\frac{Du}{Dt} - fv + g' \frac{\partial h}{\partial x} = \frac{A_H}{H} \nabla \cdot (H \nabla u), \quad (8)$$

$$\frac{Dv}{Dt} + fu + g' \frac{\partial h}{\partial y} = \frac{A_H}{H} \nabla \cdot (H \nabla v), \quad (9)$$

and

$$\frac{Dh}{Dt} + H \left( \frac{\partial u}{\partial x} + \frac{\partial v}{\partial y} \right) = 0. \quad (10)$$

[22] The notations are conventional with  $u$  and  $v$  as the zonal and meridional velocities, respectively.  $g' (= \Delta\rho g/\rho_0)$  is the reduced gravity and  $H (= H_o + h)$  is the total

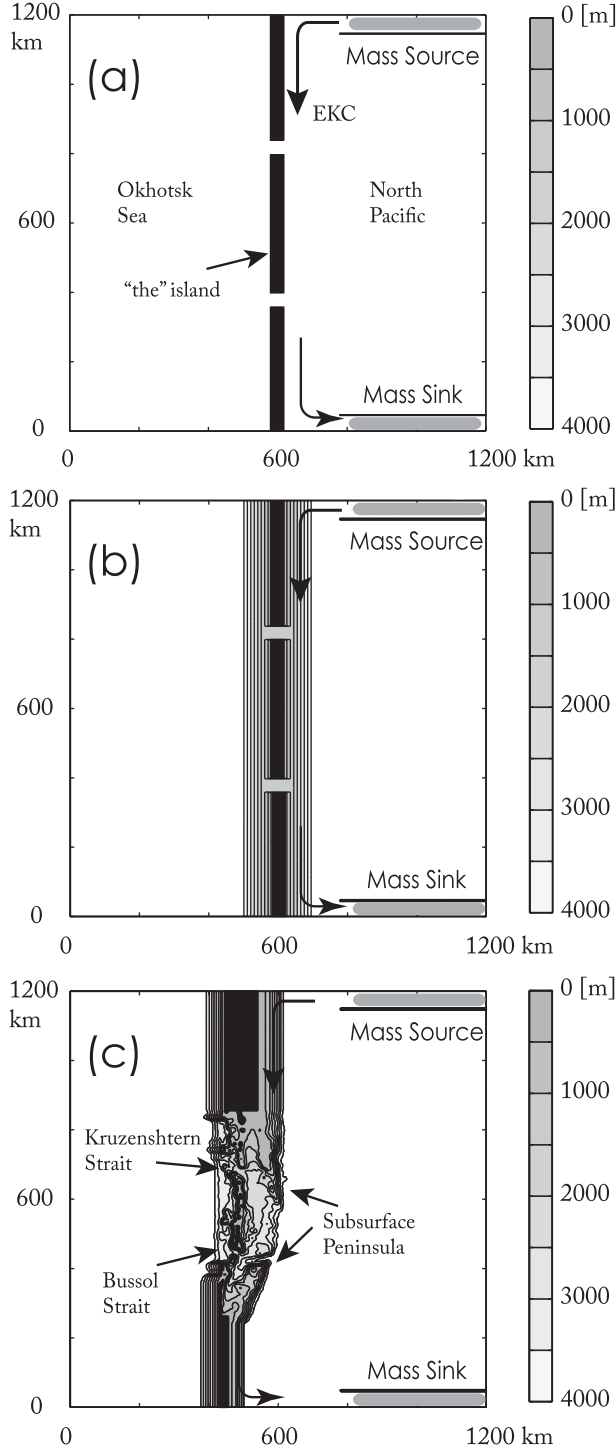


**Figure 4.** Bottom topography of the model experiments used in (a) CTRL and NCTRL (b) SLOPE, and (c) RTOPO. EKC is forced by a mass source/sink.

thickness of the layer, where  $H_0$  is the mean thickness and  $h$  is its deviation. Following *Katsumata and Yasuda* [2010] and *Yasuda* [1997], the  $\sigma_\theta = 27.5$  isopycnal is chosen as the bottom interface of the water mass exchange with  $g' = 0.01$  and  $H_0 = 1000$  m.  $A_H$  is the horizontal viscosity coefficient set to  $200 \text{ m s}^{-2}$ . Coriolis parameter  $f$  is represented by a  $\beta$ -plane with  $f = 1.2 \times 10^{-4} \text{ s}^{-1}$  at the center latitude of the domain and  $\beta = 2 \times 10^{-11} \text{ m}^{-1} \text{ s}^{-1}$ .

[23] The model domain is set to that shown in Figure 4a. It is a square basin of 1200 km with a resolution of 2 km. The Okhotsk Sea and the North Pacific are separated by a wall that mimics the Kuril island chain at  $x = 600$  km with two straits and an island in between. This island will be referred to as “the” island hereafter. The EKC is forced by prescribing a mass source/sink of  $Q$  at the northern/southern boundaries of the North Pacific. The regions close to these mass source/sink are set viscous ( $A_H = 1000 \text{ m s}^{-2}$ ) and are surrounded by a wall so that the formation of  $\beta$ -plumes [*Kida et al.*, 2008] can be avoided. No-slip and no-normal flow conditions are used along at the solid boundaries.

[24] The model parameters are set close to those observed:  $Q = 10 \text{ Sv}$ ,  $L_x = 30 \text{ km}$ ,  $L_y = 300 \text{ km}$ , and  $l = 40 \text{ km}$ . The role of inertia is neglected at first by excluding the advection terms and setting  $H$  to  $H_0$  in equations (8–10), thus a linear 1.5-layer model. This experiment will be referred to as the control experiment (CTRL) hereafter (Table 1). We will vary the model parameters from CTRL to test how well equation (4) explains the sensitivity of the exchange flow. The impact of inertia will be examined by setting the model parameters identical to CTRL but with the full equations of equations (8–10). This experiment will be referred to as NCTRL.

### 3.2. Two-Layer Isopycnal Model

[25] Hallberg isopycnal model (HIM) is used [*Hallberg*, 1997] for the two-layer isopycnal model. All model parameters are set identical to the 1.5-layer reduced gravity model, such as spatial resolution, reduced gravity, and lateral viscosity. The major differences from the 1.5-layer model are the inclusion of an active lower layer, barotropic dynamics, and bottom topography. No external forcing is applied to the lower layer. The model can handle vanishing layer thickness and the initial interface is set to 1000 m but is absent where the bathymetry is shallower.

[26] We will pursue two kinds of experiments using HIM. One has an idealized continental slope, which will be referred to as SLOPE (Figure 4b). SLOPE has a constant slope of 0.05, a representative value of the region. The bathymetry is 100 m deep at the coastline of the island chain but becomes 4000 m deep in the interior. The depths of the two straits are 1000 m. Another experiment has a realistic bathymetry based on the *ETOPO2v2* [2006] data set but with the island chain slightly rotated so that they align meridionally. This experiment will be referred to as RTOPO (Figure 4c).

## 4. Simulated Exchange Flow and its Sensitivity to Model Parameters

### 4.1. The Control Experiment

[27] The 1.5-layer model is initially at rest and is integrated for 8 years. It takes about 6 years for the linear model to reach a steady state and the flow field on the last day of year 8 is presented here.

[28] CTRL simulates an exchange flow of 6.4 Sv and a western boundary current of 3.6 Sv (Figure 5a). The magnitude of this exchange transport is somewhat larger than observations but nonetheless, the general circulation pattern that establishes in the model is analogous to

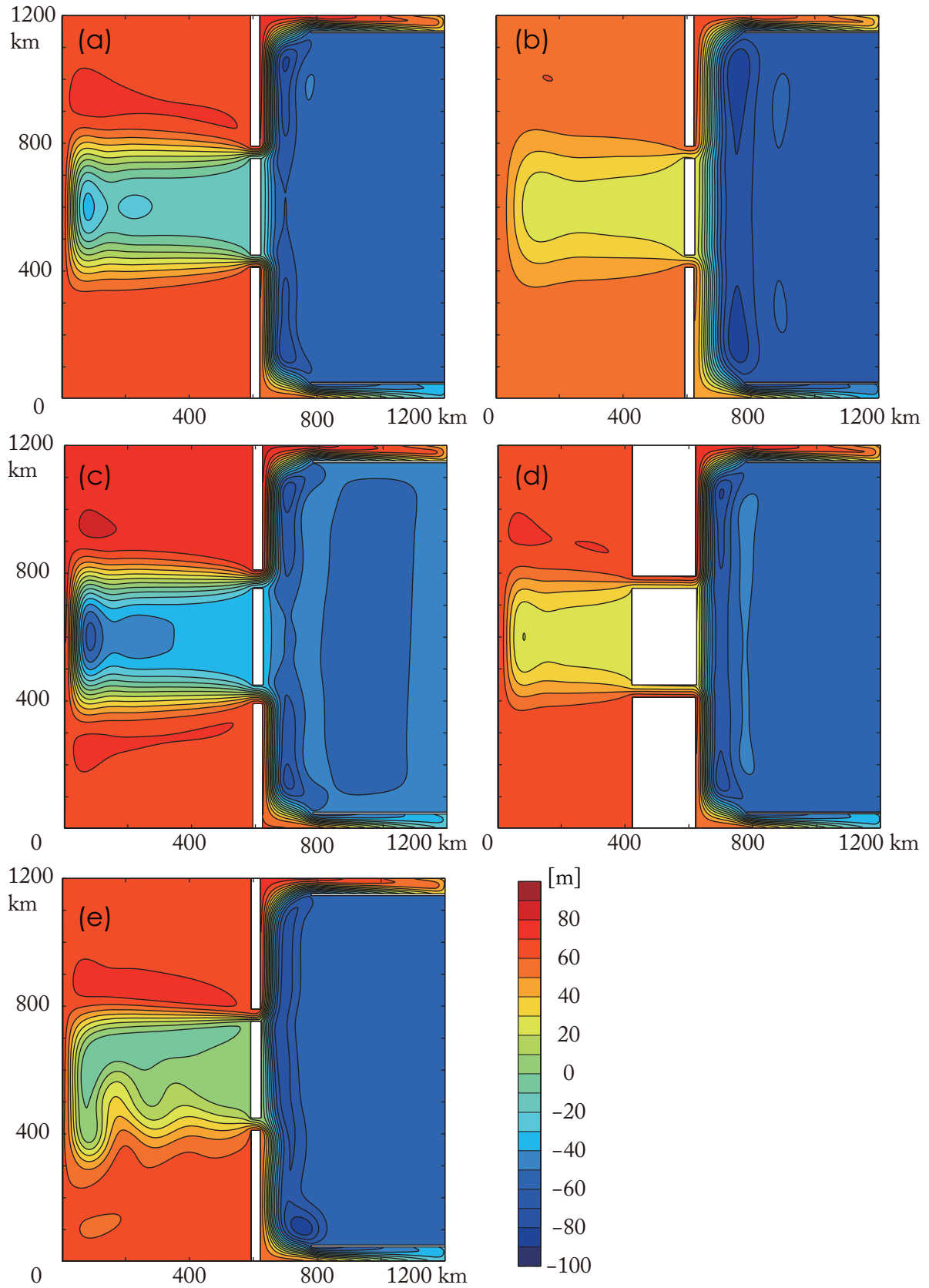


**Figure 5.** Simulated thickness perturbation contoured every 5 m. (a) CTRL. Linear model results where parameters are varied from CTRL: (b)  $A_H = 1000 \text{ m}^2 \text{ s}^{-1}$ , (c)  $l = 60 \text{ km}$ , and (d)  $L_X = 200 \text{ km}$ . (e) NCTRL.

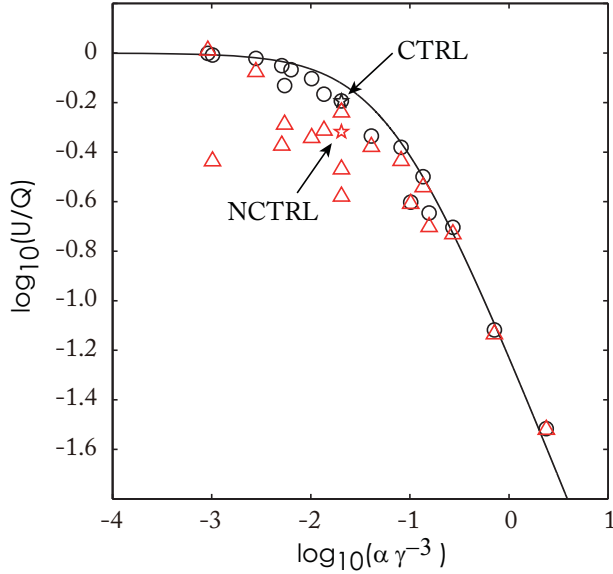


**Figure 6.** The sensitivity of the nondimensionalized exchanged transport,  $U/Q$ , to the nondimensional parameter,  $\alpha \cdot \gamma^{-3}$ . The solid line is equation (4). Black circles are from the linear model and the star is CTRL. Red triangles are from the nonlinear model and the red star is NCTRL.

observations and suggests that the EKC is capable of driving an exchange flow across the Kuril island chain. The circulation that establishes in the Okhotsk Sea is cyclonic. It flows zonally from the Kruzenshtern strait to the western boundary, turns south, and then flows zonally toward the Bussol strait. The flow is basically flowing along the background potential vorticity (PV) contours except at the western boundary. The magnitude of the exchange transport matches reasonably well with that estimated from equation (4), which is 8.0 Sv. The exchange flows have parabolic velocity profiles across the straits, similar to the assumption made when deriving equation (4), and the western boundary current has a width of the Munk boundary layer. CTRL support that equation (4) is a reasonable measure for estimating the exchange transport.

#### 4.2. Sensitivity of the Exchange Flow to Island Geometry, Width of the Straits, and Friction

[29] When  $A_H$ ,  $Q$ ,  $l$ , and  $L_x$  are varied from CTRL, equation (4) is found to represent the sensitivity of the exchange transport well (Figure 6). For example, when  $A_H$  is increased to  $1000 \text{ m}^2 \text{ s}^{-1}$ ,  $\gamma$  decreases and  $U$  decreases to 2.5 Sv (Figure 5b). Larger  $A_H$  creates broader western boundary layer while the shear within the strait remains fixed, so a smaller  $U$  is needed to achieve the same frictional stress exerted by  $V$ . When  $l$  is increased to 60 km,  $\gamma$  increases and  $U$  increases to 8.6 Sv (Figure 5c). Wider strait decreases the shear within the strait, so a larger  $U$  is needed to balance the frictional stress exerted by  $V$ . When  $L_x$  is increased to 200 km,  $\alpha$  increases and  $U$  decreases to 3.2 Sv (Figure 5d). Since the length scale of the frictional stress exerted along the straits increases, a smaller  $U$  is needed to balance that exerted by  $V$ . In contrast, when  $L_x$  is very small (8 km) we find  $U$  to increase and become close to  $Q$  (not shown). With less frictional stress exerted along

the straits, less  $V$  is induced and most of the EKC becomes the exchange flow ( $U \sim Q$ ). This solution matches equation (4) when  $\alpha$  is taken to zero.

[30] Estimates of the frictional stress along the island further confirm that the Circulation theorem holds in various experiments. In CTRL, the frictional stress exerted by the exchange flow and the western boundary current are  $-0.024$  and  $0.025 \text{ m}^2 \text{ s}^{-2}$ , respectively, while that along the western coast is less than  $-0.001 \text{ m}^2 \text{ s}^{-2}$  and secondary. The sum of the frictional stress is indeed zero and the main balance is that between the exchange flow and the western boundary current. When  $A_H = 1000 \text{ m}^2 \text{ s}^{-1}$  (Figure 5b), the frictional stresses exerted by the exchange flow and the western boundary current increase to  $-0.51$  and  $0.53 \text{ m}^2 \text{ s}^{-2}$ , respectively. Although the exchange transport decreases to 2.5 Sv compared to CTRL, the main balance of frictional stress between the exchange flow and the western boundary current remains the same. Model results support the hypothesis that the Circulation theorem explains the dynamics of the EKC-driven exchange flow well and that equation (4) provides a reasonable estimate of its transport.

#### 4.3. The Role of Inertia

[31] We examine now the role of inertia using NCTRL. It takes about 6 years for the 1.5-layer nonlinear model to reach a quasi-steady state and the averaged flow field of year 8 is presented here.

[32] The exchange flow simulated in NCTRL is 4.8 Sv (Figure 5e). This is less than CTRL and that estimated from equation (4). When various parameters are varied from NCTRL, we find the nonlinear model to generally show less transport compared to that simulated in the linear model and equation (4) (Figure 6). The presence of inertia appears to reduce the magnitude of  $U$ . This reduction in  $U$  in the presence of inertia qualitatively matches with the results of *Sheremet* [2001] where more western boundary

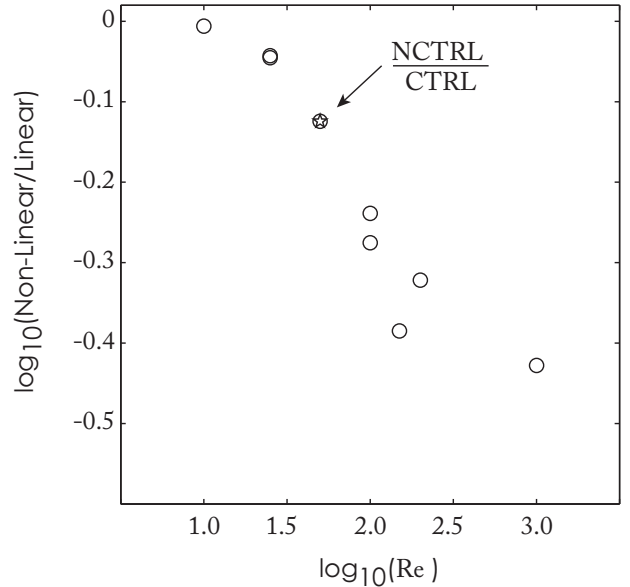


**Figure 7.** The ratio of the exchange transports simulated in nonlinear models compared to that in linear models and its dependence with the Reynolds number.

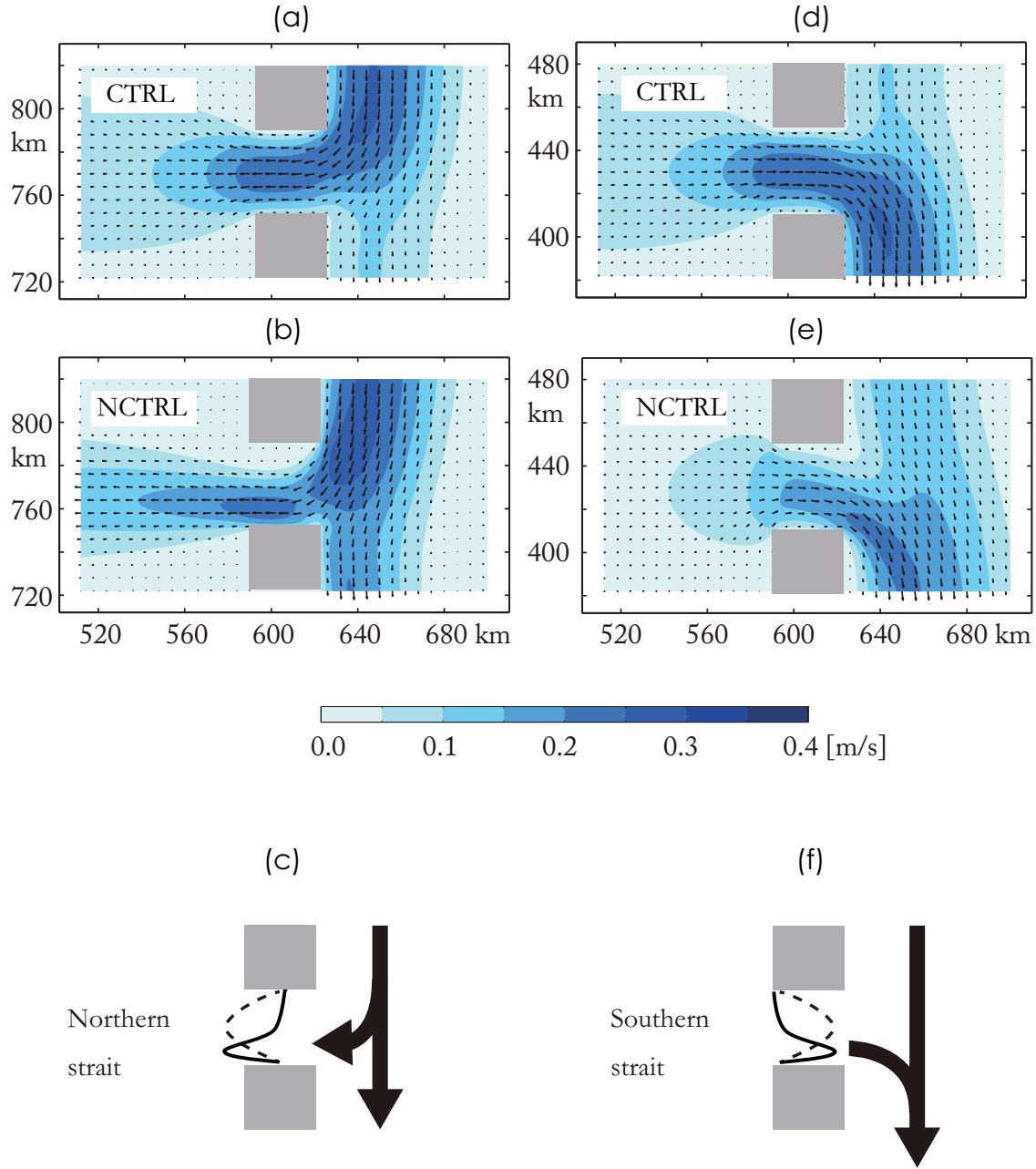


**Figure 8.** (a–c) The flow field and speed near the northern strait. (a) CTRL, (b) NCTRL, and (c) a schematic of the zonal velocity profile in the strait. The dotted line is CTRL and thin solid line is NCTRL. (d–f) The flow field and speed near the southern strait. (d) CTRL, (e) NCTRL, and (f) a schematic of the zonal velocity profile in the strait.

current is found to leap across a strait in the presence of inertia and not enter a marginal sea. When the impact of inertia is measured using the Reynolds number ( $Re = Q / (A_H / H_0)$ ) following Sheremet [2001], the reduction of  $U$  compared to the linear model is indeed found to increase as  $Re$  increases (Figure 7). Note that in order to focus on the sensitivity to  $Re$ , only the experiments where  $Q$  and  $A_H$  are varied from CTRL and NCTRL are shown. Model results suggest that the estimate based on equation (4) serves like an upper limit of the exchange transport.

[33] Why does the exchange transport reduce when inertia is present? We will try to explain this from the Circula-

tion theorem since it does not depend on linearity. Equation (1') suggests that the transport of the western boundary transport cannot increase alone because that will only increase the frictional stress exerted along the eastern coast of the island and make the sum of frictional stresses go nonzero. What we find in NCTRL is that the frictional stress along the northern coast of the island increases significantly (Figures 8a and 8b): from  $-0.013 \text{ m}^2 \text{ s}^{-2}$  in CTRL to  $-0.044 \text{ m}^2 \text{ s}^{-2}$  in NCTRL. Frictional balance is achieved primarily between the stresses along the northern coast and the eastern coast ( $0.055 \text{ m}^2 \text{ s}^{-2}$ ). Frictional stress along the southern coast becomes secondary ( $0.004 \text{ m}^2$

$s^{-2}$ ) (Figures 8d and 8e). These changes occur because the northern and southern boundary layer widths change in the presence of inertia. With a southward momentum of the EKC, the northern boundary layer is squeezed while the southern boundary layer is stretched (Figures 8c and 8f). The velocity shear and frictional stress thus increase along the northern boundary while they decrease along the southern boundary. The island's western boundary current will balance the enhanced friction along the northern coast by increasing its transport.

[34] The frictional balance of NCTRL suggests inertia will modify equation (4) as well. The frictional stress along the southern coast (the last term in equation (2)), which is part of the frictional balance considered when deriving equation (4), is no longer significant when inertia is strong. The spatial scale of the velocity shear in the northern strait is also no longer  $l/2$ . Equation (2) is thus better expressed as:

$$0 = A_H \left( \frac{U/(H_0 \cdot \delta_N)}{\delta_N^2} L_x + \frac{(-V)/(H_0 \cdot \delta_M)}{\delta_M^2} L_y \right), \quad (11)$$

where  $\delta_N$  is the width of exchange flow along the northern coast. Using  $Q = U + V$ , equation (11) becomes

$$U = \frac{Q}{1 + \alpha \left( \frac{\delta_N}{\delta_M} \right)^{-3}}. \quad (12)$$

Equation (12) shows that  $U$  will decrease as inertia decreases  $\delta_N$ . When comparing equation (12) to equation (4), the role of inertia is found to be analogous to narrowing the straits in equation (4).

## 5. The Impact of the Continental Slopes and Topographic Features

[35] The actual Kuril island chain is accompanied by continental slopes and complex topographic features. Continental slopes can act as a PV barrier and restrict open oceanic flows from entering the strait [Yang *et al.*, 2013]. Friction is required for the western boundary current to cross this PV barrier before inducing an exchange flow. Yang *et al.* [2013] focus on the impact of continental slopes on the Island rule so a western boundary current from the upstream is absent. Here, we will focus on how continental slopes and topographic features may affect the EKC-driven exchange flow using SLOPE and RTOPO. It takes about 6 years for these model experiments to reach a steady state and the averaged flow field of year 8 is presented here, just like NCTRL.

### 5.1. The Impact of Continental Slopes

[36] In SLOPE, we find an exchange transport of 5.0 Sv (Figure 9a), which is similar to NCTRL. The basic flow field is similar to that in NCTRL (Figure 8b) and the presence of a steep slope appears to affect the exchange transport only moderately (Figure 9b). This is likely because the region that is affected by the slope lies within the Munk boundary layer (about 21 km). With a slope of 0.05, the 1000 m isobath (the depth of the straits) exists about 18 km

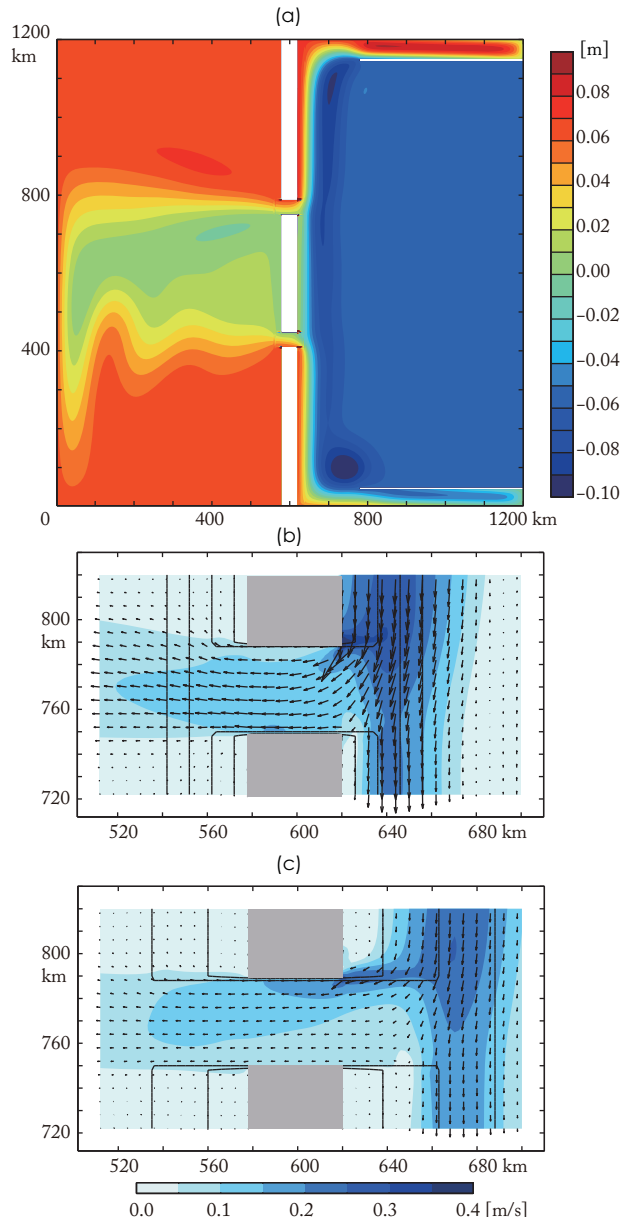


**Figure 9.** The flow field simulated in SLOPE. (a) The sea surface height (SSH). (b) The flow field near the northern strait in SLOPE. Color contours show the flow speed. Bathymetric contours are drawn every 500 m. (c) The flow field near the northern strait when the continental slope is 0.02.

from the coast. While the slope can change the background PV contour and make the EKC flow along the bathymetric contours, the experiment shows that the presence of a steep slope does not change the width of the EKC much and significantly alter the exchange flow from that without a slope.

[37] Further experiments suggest that continental slopes can affect the exchange flow if the slope is less steep. This is because a moderate slope will change PV contours near the coast such that the majority of the EKC will flow outside the Munk boundary layer and not touch the island. For example, when the slope is 0.02, the 1000 m isobath lies outside the Munk boundary layer and part of the EKC that

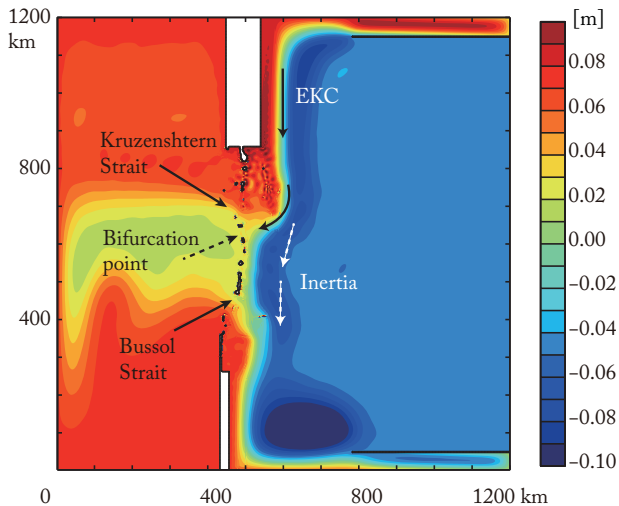


**Figure 10.** The time-averaged SSH and flow field in RSLOPE. The EKC bifurcates between the Kruzshstern and Bussol straits. The white arrows show the pathway of the EKC when inertia increases.

flows in deeper depths than the strait ( $>1000$  m) will continue to flow southward across the strait far from the island coastline (Figure 9c). With no frictional stress exerted along the island, an exchange flow is not induced. Part of the EKC that flows in shallower depth ( $<1000$  m) enters the strait but aligns along the northern side of the strait and exerts much less frictional stress along the island. The role of frictional stresses around an island on inducing the exchange flow appears much reduced. What the model shows is that if the continental slope is moderate, the magnitude of the exchange flow depends more strongly on how much of the EKC exists in shallow depths prior to encountering the strait.

[38] The reduction in the exchange flow that we find for moderate slopes is qualitatively similar to the role of topography found in *Yang et al.* [2013]. For a realistic EKC, however, the steep slopes of the Kamchatka Peninsula and the deep straits of the Kuril island chain likely enable the EKC to flow across the PV barrier within a short distance and establish a boundary current and exchange flows similar to NCTRL. The impact of the topography is likely weaker in our study because part of the EKC already exists in the upstream against the coastline prior to encountering the strait. The PV barrier to cross the straits for such an along-coastline flow is much reduced. Around the Kuril island chain, the depth of the straits (1000 m) is also close to the depth of the isopycnal interface intersecting the bottom ( $\sim 1200$  m), so the PV barrier that the EKC needs to overcome is not as significant as that for shallower straits.

[39] SLOPE suggests that the basic dynamics of the EKC-driven exchange flow remains similar to NCTRL as long as the continental slope is steep and the straits are deep. The continental slopes of the Kuril island chain are therefore likely to play a minor role on the dynamics of the exchange flow.

## 5.2. The Impact of a Subsurface Peninsula

[40] In RTOPO, we find an exchange transport of 4.1 Sv (Figure 10), which is about 1–3 Sv less than the previous

experiments. Detailed topographic features of the Kuril island chain appear to affect the magnitude of the transport significantly.

[41] One reason why the exchange transport reduces in RTOPO from NCTRL could be that the strait is no longer rectangular. With a more parabolic shape, the total area of the strait is smaller. However, we consider the main reason to be the changes in  $L_x$  and  $L_y$ , the length scales of the frictional stress induced by the exchange flow and the western boundary current, respectively. In RTOPO, the distance between the Kruzshstern and Bussol straits is about 230 km, which is shorter than 300 km previously used for  $L_y$ . Moreover, the presence of a subsurface peninsula makes the EKC bifurcate along the eastern coast of the island between the two straits (Figure 10). So the actual length scale of the western boundary current that travels southward along the island is that between this bifurcation point and the Bussol strait, which is about 200 km. On the other hand, the distance from the bifurcation point to the Kruzshstern strait increases to 60 km compared to 30 km previously used for  $L_x$ . These changes increase  $\alpha$  (in equation (4)) to 0.3 compared to 0.1 in CTRL and based on equation (4), such increase would reduce the exchange transport about 2.3 Sv, which matches with the order of the reduction observed from CTRL, NCTRL, and RTOPO.

[42] The presence of a subsurface peninsula is found to change how inertia affects the exchange flow as well. When the transport of the EKC is increased, we find more EKC to continue southward rather than turning west and encountering the island between the Kruzshstern and Bussol straits (Figure 10). As a result, the exchange flow that is driven by the EKC also reduces.

[43] RTOPO shows that detailed topographic features are capable of affecting the magnitude of the exchange flow significantly. For the Kuril island chain, the subsurface peninsula is found to limit the exchange flow by changing the bifurcation point of the EKC. It also alters the role of inertia by making the EKC flow across the subsurface peninsulas and induces less exchange flow.

## 6. Summary and Remarks

[44] What are the main processes that control the exchange flow between the Okhotsk Sea and the North Pacific? In this paper, we presented how the EKC may drive an exchange flow based on Kelvin’s Circulation theorem around an island that is located between the Kruzshstern strait and the Bussol strait. A scaling estimate of the exchange transport was further derived (equation (4)) by assuming that the frictional stresses exerted by the exchange flow and the EKC east of the island balance.

[45] Numerical experiments based on a 1.5-layer reduced gravity model revealed that equation (4) quantified the dynamics of the exchange transport well. The exchange transport was found sensitive not only to the width of the strait but also to the magnitude of friction and the aspect ratio of the island geometry. The role of inertia was found to decrease the exchange transport by enhancing the frictional stress exerted along the Kruzshstern strait.

[46] The impact of the continental slope was found to be minor. As long as the straits are deep and the slopes are as steep as that found along the Kuril island chain, the

presence of continental slopes are unlikely to significantly alter the dynamics of the exchange flow. On the other hand, the detailed topographic features of the Kuril island chain were found to affect the magnitude of the exchange transport significantly. The presence of a subsurface peninsula is likely responsible for such impact since it makes the EKC bifurcate along the eastern coast of the island. This results in changing the length scale of the frictional stresses exerted by the exchange flow and the western boundary current. The subsurface peninsula also enabled inertia to make the EKC flow away from the island and to induce less exchange flow.

[47] Our idealized model study suggests that simulating the exchange flow between the Okhotsk Sea and the North Pacific in a GCM is likely to depend not only on resolving the widths of the Kruzenshtern and Bussol straits but also on how well the EKC is simulated. Detailed topography as well as the magnitude of the subgrid-scale eddy-viscosity will strongly influence the exchange transport and thus, need careful attention. Selecting a proper lateral viscosity coefficient near the western boundary current is beyond the scope of this study, but the dependence of the exchange flow on this parameter points to the complexity of the dynamics governing the exchange flow. The basic mechanism of the EKC-driven exchange flow presented in this work is likely applicable to other locations where the marginal sea-open ocean exchange flow occur as well. The presence of western boundary currents and narrow straits bounding an island are the key requirements. While the mechanism successfully explains why the Island rule [Godfrey, 1989] overestimates the exchange transport between the Okhotsk Sea and the North Pacific [Katsumata and Yasuda, 2010; Ohshima et al., 2010], the impact of time variability is yet to be explored. We plan to investigate this problem next.

[48] **Acknowledgments.** The authors thank two anonymous reviewers for many useful comments. This study benefitted from the collaborative research program of the Institute of Low Temperature Science at Hokkaido University. S. Kida was supported by KAKENHI (22106002) and B. Qiu by NSF (OCE-0926594).

## References

- Durland, T. S., and B. Qiu (2003), Transmission of subinertial Kelvin waves through a strait, *J. Phys. Oceanogr.*, *33*(7), 1337–1350.
- ETOPO2v2 (2006), 2-minute Gridded Global Relief Data (ETOPO2v2), Natl. Oceanic and Atmos.c Admin., Natl. Geophys. Data Cent., U.S. Dep. of Commer, Boulder, Colo. [Available at <http://www.ngdc.noaa.gov/mgg/fliers/06mvg01.html>.]
- Godfrey, J. S. (1989), A Sverdrup model of the depth-integrated flow for the world ocean allowing for island circulations, *Geophys. Astrophys. Fluid Dyn.*, *45*, 89–112.
- Hallberg, R. (1997), Stable split time stepping schemes for large scale ocean modeling, *J. Comput. Phys.*, *135*, 54–65.
- Katsumata, K., and I. Yasuda (2010), Estimates of non-tidal exchange transport between the sea of Okhotsk and the North Pacific, *J. Oceanogr.*, *66*(4), 489–504, doi:10.1007/s10872-010-0041-9.
- Katsumata, K., I. Yasuda, and Y. Kawasaki (2001), Direct current measurements at Kruzenshterna Strait in summer, *Geophys. Res. Lett.*, *28*(2), 319–322.
- Katsumata, K., K. I. Ohshima, T. Kono, M. Itoh, I. Yasuda, Y. N. Volkov, and M. Wakatsuchi (2004), Water exchange and tidal currents through the Bussol Strait revealed by direct current measurements, *J. Geophys. Res.*, *109*, C09S06, doi:10.1029/2003JC001864.
- Kida, S., J. F. Price, J. Yang (2008), The Upper-Oceanic Response to Overflows: A Mechanism for the Azores Current, *J. Phys. Oceanogr.*, *38*, 880–895, doi: 10.1175/2007JPO3750.1.
- Nakamura, T., and T. Awaji (2004), Tidally induced diapycnal mixing in the Kuril Straits and its role in water transformation and transport: A three-dimensional nonhydrostatic model experiment, *J. Geophys. Res.*, *109*, C09S07, doi:10.1029/2003JC001850.
- Nishioka, J., et al. (2007), Iron supply to the western subarctic Pacific: Importance of iron export from the Sea of Okhotsk, *J. Geophys. Res.*, *112*, C10012, doi:10.1029/2006JC004055.
- Nof, D. (1995), Choked flows from the Pacific to the Indian Ocean, *J. Phys. Oceanogr.*, *25*(6), 1369–1383.
- Ohshima, K. I., T. Nakanowatari, S. Riser, and M. Wakatsuchi (2010), Seasonal variation in the in- and outflow of the Okhotsk Sea with the North Pacific, *Deep Sea Res., Part II*, *57*, 1247–1256, doi:10.1016/j.dsr2.2009.12.012.
- Pedlosky, J. (1994), Ridges and recirculations: Gaps and jets, *J. Phys. Oceanogr.*, *24*(12), 2703–2707.
- Pedlosky, J. (1996), *Ocean Circulation Theory*, pp. 38–43, Springer, Berlin.
- Pedlosky, J., L. J. Pratt, M. A. Spall, and K. R. Helfrich (1997), Circulation around islands and ridges, *J. Mar. Res.*, *55*(6), 1199–1251.
- Pratt, L., and J. Pedlosky (1998), Barotropic circulation around Islands with friction, *J. Phys. Oceanogr.*, *28*, 2148–2162, doi:10.1175/1520-0485(1998)028<2148:BCAIWF>2.0.CO;2.
- Pratt, L. J., and M. A. Spall (2003), A porous-medium theory for barotropic flow through ridges and archipelagos, *J. Phys. Oceanogr.*, *33*, 2702–2718.
- Risien, C. M., and D. B. Chelton (2008), A global climatology of surface wind and wind stress fields from eight years of QuikSCAT scatterometer data, *J. Phys. Oceanogr.*, *38*, 2379–2413, doi: 10.1175/2008JPO3881.1.
- Sheremet, V. A. (2001), Hysteresis of a western boundary current leaping across a gap, *J. Phys. Oceanogr.*, *31*, 1247–1259, doi:10.1175/1520-0485(2001)031<1247:HOAWBC>2.0.CO;2.
- Talley, L. D. (1993), Distribution and formation of the North Pacific intermediate water, *J. Phys. Oceanogr.*, *23*, 517–537.
- Verkhunov, A. V., and Y. Y. Tkachenko (1992), Recent observations of variability in the western Bering Sea current system, *J. Geophys. Res.*, *97*(C9), 14,369–14,376.
- Yang, J., X. Lin, and D. Wu (2013), Wind-driven exchanges between two basins: Some topographic and latitudinal effects, *J. Geophys. Res.*, *118*, 4585–4599, doi:10.1002/jgrc.20333.
- Yasuda, I. (1997), The origin of the North Pacific intermediate water, *J. Geophys. Res.*, *102*(C1), 893–909, doi:10.1029/96JC02938.
- Yasuda, I., et al. (2002), Influence of Okhotsk Sea intermediate water on the Oyashio and North Pacific intermediate water, *J. Geophys. Res.*, *107*(C12), 3237, doi:10.1029/2001JC001037.